WCAP 10554

TECHNICAL BASES FOR ELIMINATING LARGE PRIMARY LOOP PIPE RUPTURE AS THE STRUCTURAL DESIGN BASIS FOR BYRON UNITS 1 AND 2 AND BRAIDWOOD UNITS 1 AND 2

MAY, 1984

S. A. Swamy
R. [illegible]urner
H. F. Clark, Jr.
R. A. Holmes
W. H. Bamford
Y. S. Lee

APPROVED: _____
J. N. Chirigos, Mgr.
Structural Materials
Engineering

APPROVED: _____
E. R. Johnson, Mgr.
Structural and Seismic
Development

APPROVED: _____
J. J. McInerney, Mgr.
Mechanical Equipment
and Systems Licensing

WESTINGHOUSE ELECTRIC CORPORATION
NUCLEAR ENERGY SYSTEMS
P.O. BOX 355
PITTSBURGH, PENNSYLVANIA 15230

FOREWORD

This document contains Westinghouse Electric Corporation proprietary information and data which has been identified by brackets. Coding associated with the brackets set forth the basis on which the information is considered proprietary. These codes are listed with their meanings in WCAP-7211.

The proprietary information and data contained in this report were obtained at considerable Westinghouse expense and its release could seriously affect our competitive position. This information is to be withheld from public disclosure in accordance with the Rules of Practice, 10 CFR 2.790 and the information presented herein be safeguarded in accordance with 10 CFR 2.903. Withholding of this information does not adversely affect the public interest.

This information has been provided for your internal use only and should not be released to persons or organizatons outside the Directorate of Regulation and the ACRS without the express written approval of Westinghouse Electric Corporation. Should it become necessary to release this information to such persons as part of the review procedure, please contact Westinghouse Electric Corporation, which will make the necessary arrangements required to protect the Corporation's proprietary interests.

The proprietary information is deleted in the unclassified version of this report.

TABLE OF CONTENTS

LIST OF TABLES

LIST OF FIGURES

1.0 INTRODUCTION

1.1 Purpose

This report applies to the Byron/Braidwood plants reactor coolant system primary loop piping. It is intended to demonstrate that specific parameters for the Byron/Braidwood plants are enveloped by the generic analysis performed by Westinghouse in WCAP-9558, Revision 2 (Reference 1) and accepted by the NRC (Reference 2).

1.2 Scope

The current structural design basis for the Reactor Coolant System (RCS) primary loop requires that pipe breaks be postulated as defined in the approved Westinghouse Topical Report WCAP-8082 (Reference 3). In addition, protective measures for the dynamic effects associated with RCS primary loop pipe breaks have been incorporated in the Byron/Braidwood plants design. However, Westinghouse has demonstrated on a generic basis that RCS primary loop pipe breaks are highly unlikely and should not be included in the structural design basis of Westinghouse plants (see Reference 4). In order to demonstrate this applicability of the generic evaluations to the Byron/Braidwood plants, Westinghouse has performed: a comparison of the loads and geometry for the Byron/Braidwood plants with envelope parameters used in the generic analyses (Reference 1), a fracture mechanics evaluation, a determination of leak rates from a through-wall crack, fatigue crack growth evaluation, and an assessment of margins.

1.3 Objectives

The conclusions of WCAP-9558, Revision 2 (Reference 1) support the elimination of RCS primary loop pipe breaks for the Byron/Braidwood plants. In order to validate this conclusion the following objectives must be achieved.

a. Demonstrate that Byron/Braidwood plants parameters are enveloped by generic Westinghouse studies.

b. Demonstrate that margin exists between the critical crack size and a postulated crack which yields a detectable leak rate.

c. Demonstrate that there is sufficient margin between the leakage through a postulated crack and the leak detection capability of the Byron/Braidwood plants.

d. Demonstrate that fatigue crack growth is negligible.

1.4 Background Information

Westinghouse has performed considerable testing and analysis to demonstrate that RCS primary loop pipe breaks can be eliminated from the structural design basis of all Westinghouse plants. The concept of eliminating pipe breaks in the RCS primary loop was first presented to the NRC in 1978 in WCAP-9283 (Reference 5). This Topical Report employed a deterministic fracture mechanics evaluation and a probabilistic analysis to support the elimination of RCS primary loop pipe breaks. The approach was then used as a means of addressing Generic Issue A-2 and Asymmetric LOCA Loads.

Westinghouse performed additional testing and analysis to justify the elimination of RCS primary loop pipe breaks. As a result of this effort, WCAP-9558, Revision 2; WCAP-9787, and Letter Report NS-EPR-2519 (References 1, 6, and 7) were submitted to the NRC.

The NRC funded research through Lawrence Livermore National Laboratory (LLNL) to address this same issue using a probabilistic approach. As part of the LLNL research effort, Westinghouse performed extensive evaluations of specific plant loads, material properties, transients, and system geometries to demonstrate that the analysis and testing previously performed by Westinghouse and the research performed by LLNL applied to all Westinghouse plants, including Byron/Braidwood (References 8 and 9). The results from the LLNL

study were released at a March 28, 1983 ACRS Subcommittee meeting. These studies which are applicable to all Westinghouse plants east of the Rocky Mountains, determined the mean probability of a direct LOCA (RCS primary loop pipe break) to be 10^{-10} per reactor year and the mean probability of an indirect LOCA to be 10^{-7} per reactor year. Thus, the results previously obtained by Westinghouse (Reference 5) were confirmed by an independent NRC research study.

Based on the studies by Westinghouse, by LLNL, the ACRS, and the AIF, the NRC completed a safety review of the Westinghouse reports submitted to address asymmetric blowdown loads that result from a number of discrete break locations on the PWR primary systems. The NRC Staff evaluation (Reference 2) concludes that an acceptable technical basis has been provided so that asymmetric blowdown loads need not be considered for those plants that can demonstrate the applicability of the modeling and conclusions contained in the Westinghouse response or can provide an equivalent fracture mechanics demonstration of the primary main coolant loop integrity.

This report will demonstrate the applicability of the Westinghouse generic evaluations to the Byron/Braidwood plants.

2.0 OPERATION AND STABILITY OF THE REACTOR COOLANT SYSTEM

The Westinghouse reactor coolant system primary loop has an operating history which demonstrates its inherent stability characteristics of the design. This includes a low susceptibility to cracking failure from the effects of corrosion (e.g., intergranular stress corrosion cracking), water hammer, or fatigue (low and high cycle). This operating history totals over 400 reactor-years, including five plants each having 15 years of operation and 15 other plants each with over 10 years of operation.

2.1 Stress Corrosion Cracking

For the Westinghouse plants, there is no history of cracking failure in the reactor coolant system loop piping. For stress corrosion cracking (SCC) to occur in piping, the following three conditions must exist simultaneously: high tensile stresses, a susceptible material, and a corrosive environment (Reference 10). Since some residual stresses and some degree of material susceptibility exist in any stainless steel piping, the potential for stress corrosion is minimized by proper material selection immune to SCC as well as preventing the occurrence of a corrosive environment. The material specifications consider compatibility with the system's operating environment (both internal and external) as well as other materials in the system, applicable ASME Code rules, fracture toughness, welding, fabrication, and processing.

The environments known to increase the susceptibilty of austenitic stainless steel to stress corrosion are (Reference 10): oxygen, fluorides, chlorides, hydroxides, hydrogen peroxide, and reduced forms of sulfur (e.g., sulfides, sulfites, and thionates). Strict pipe cleaning standards prior to operation and careful control of water chemistry during plant operation are used to prevent the occurrence of a corrosive environment. Prior to being put into service, the piping is cleaned internally and externally. During flushes and preoperational testing, water chemistry is controlled in accordance with written specifications. External cleaning for Class 1 stainless steel piping includes patch tests to monitor and control chloride and fluoride levels. For

preoperational flushes, influent water chemistry is controlled. Requirements on chlorides, fluorides, conductivity, and pH are included in the acceptance criteria for the piping.

During plant operation, the reactor coolant water chemistry is monitored and maintained within very specific limits. Contaminant concentrations are kept below the thresholds known to be conducive to stress corrosion cracking with the major water chemistry control standards being included in the plant operating procedures as a condition for plant operation. For example, during normal power operation, oxygen concentration in the RCS is expected to be less than 0.005 ppm by controlling charging flow chemistry and maintaining hydrogen in the reactor coolant at specified concentrations. Halogen concentrations are also stringently controlled by maintaining concentrations of chlorides and fluorides within the specified limits. This is assured by controlling charging flow chemistry and specifying proper wetted surface materials.

2.2 Water Hammer

Overall, there is a low potential for water hammer in the RCS since it is designed and operated to preclude the voiding condition in normally filled lines. The reactor coolant system, including piping and primary components, is designed for normal, upset, emergency, and faulted condition transients. The design requirements are conservative relative to both the number of transients and their severity. Relief valve actuation and the associated hydraulic transients following valve opening are considered in the system design. Other valve and pump actuations are relatively slow transients with no significant effect on the system dynamic loads. To ensure dynamic system stability, reactor coolant parameters are stringently controlled. Temperature during normal operation is maintained within a narrow range by control rod position; pressure is controlled by pressurizer heaters and pressurizer spray also within a narrow range for steady-state conditions. The flow characteristics of the system remain constant during a fuel cycle because the only governing parameters, namely system resistance and the reactor coolant pump characteristics are controlled in the design process. Additionally, Westinghouse has instrumented typical reactor coolant systems to verify the

flow and vibration characteristics of the system. Preoperational testing and operating experience have verified the Westinghouse approach. The operating transients of the RCS primary piping are such that no significant water hammer can occur.

2.3 Low Cycle and High Cycle Fatigue

Low cycle fatigue considerations are accounted for in the design of the piping system through the fatigue usage factor evaluation to show compliance with the rules of Section III of the ASME Code. A further evaluation of the low cycle fatigue loadings was carried out as part of this study in the form of a fatigue crack growth analysis, as discussed in Section 6.

High cycle fatigue loads in the system would result primarily from pump vibrations. These are minimized by restrictions placed on shaft vibrations during hot functional testing and operation. During operation, an alarm signals the exceedance of the vibration limits. Field measurements have been made on a number of plants during hot functional testing, including plants similar to Byron/Braidwood plants. Stresses in the elbow below the RC pump have been found to be very small, between 2 and 3 ksi at the highest. These stresses are well below the fatigue endurance limit for the material, and would also result in an applied stress intensity factor below the threshold for fatigue crack growth.

3.0 PIPE GEOMETRY AND LOADING

A segment of the primary coolant cold leg pipe is shown in Figure 1. This segment is postulated to contain a circumferential through-wall flaw. The inside diameter and wall thickness of the pipe are 27.5 and 2.32 inches, respectively. The pipe is subjected to a normal operating pressure of [ ]^{a,c,e} psi. Figure 2 identifies the loop weld locations. The material properties and the loads at these locations resulting from deadweight, thermal expansion and Safe Shutdown Earthquake are indicated in Table 1. As seen from this Table, the junction of cold leg and the reactor coolant pump outlet nozzle is the worst location for crack stability analysis based on the highest stress due to combined pressure, dead weight, thermal expansion, and SSE (Safe Shutdown Earthquake) loading. At this location, the axial load (F) and the bending moment (M) are [ ]^{a,c,e} (including axial force due to pressure) and [ ]^{a,c,e}, respectively. The loads of Table 1 are calculated as follows:

The axial force F and transverse bending moments, M_y and M_z, are chosen for each static load (pressure, deadweight and thermal) based on elastic-static analyses for each of these load cases. These pipe load components are combined algebraically to define the equivalent pipe static loads F_s, M_{ys}, and M_{zs}. Based on elastic SSE response spectra analyses, amplified pipe seismic loads, F_d, M_{yd}, M_{zd} are obtained. The maximum pipe loads are obtained by combining the static and dynamic load components as follows:

$$F = |F_s| + |F_d|$$

$$M = \sqrt{M_y^2 + M_z^2}$$

where:

$$M_y = |M_{ys}| + |M_{yd}|$$

$$M_z = |M_{zs}| + |M_{zd}|$$

The corresponding geometry and loads used in the reference report (Reference 1) are as follows: inside diameter and wall thickness are 29.0 and 2.5 inches; axial load and bending moment are [ ]^{a,c,e} inch-kips. The outer fiber stress for Byron/Braidwood is [ ]^{a,c,e} ksi, while for the reference report it is [ ]^{a,c,e} ksi. This demonstrates conservatism in the reference report which makes it more severe than the Byron/Braidwood analyses.

The normal operating loads (i.e., algebric sum of pressure, deadweight, and 100 percent power thermal expansion loading) at the critical location, i.e., the junction of cold leg and the reactor coolant pump outlet nozzle are as follows:

F = [ ]^{a,c,e} (including internal pressure)
M = [ ]^{a,c,e}

The calculated and allowable stresses for ASME equation 9 (faulted) and equation 12 at the critical location are as follows:

Equation Number	Calculated Stress (ksi)	Allowable Stress (ksi)	Ratio of Calculated/ Allowable
[			] a,c,e

4.0 FRACTURE MECHANICS EVALUATION

4.1 Global Failure Mechanism

Determination of the conditions which lead to failure in stainless steel must be done with plastic fracture methodology because of the large amount of deformation accompanying fracture. A conservative method for predicting the failure of ductile material is the [

]^{a,c,e} This methodology has been shown to be applicable to ductile piping through a large number of experiments, and will be used here to predict the critical flaw size in the primary coolant piping. The failure criterion has been obtained by requiring [

]^{a,c,e} (Figure 3) when loads are applied. The detailed development is provided in Appendix A, for a through-wall circumferential flaw in a pipe with internal pressure, axial force, and imposed bending moments. The [

]^{a,c,e} for such a pipe is given by:

[ ]^{a,c,e}

where:

[ ]^{a,c,e}

[a,c,e]

The analytical model described above accurately accounts for the piping internal pressure as well as imposed axial force as they affect [ ]^{a,c,e} Good agreement was found between the analytical predictions and the experimental results (Reference 11).

4.2 Local Failure Mechanism

The local mechanism of failure is primarily dominated by the crack tip behavior in terms of crack-tip blunting, initiation, extension and finally crack instability. Depending on the material properties and geometry of the pipe, flaw size, shape and loading, the local failure mechanisms may or may not govern the ultimate failure.

The stability will be assumed if the crack does not initiate at all. It has been accepted that the initiation toughness, measured in terms of J_{IN} from a J-integral resistance curve is a material parameter defining the crack initiation. If, for a given load, the calculated J-integral value is shown to be less than J_{IN} of the material, then the crack will not initiate. If the initiation criterion is not met, one can calculate the tearing modulus as defined by the following relation:

$$T_{app} = \frac{dJ}{da} \quad \frac{E}{\sigma_f^2}$$

where:

T_{app} = applied tearing modulus
E = modulus of elasticity
σ_f = [ ]^{a,c,e} (flow stress)
a = crack length
[ ]^{a,c,e}

In summary, the local crack stability will be established by the two-step criteria:

$$J < J_{IN}$$

$$T_{app} < T_{mat} \quad \text{if } J > J_{IN}$$

4.3 Material Properties

The materials in the Byron/Braidwood Units 1 and 2 primary loops are wrought stainless steel pipe (SA 376 304N), cast stainless steel fittings (SA351 CF8A) and associated welds. The tensile and flow properties of the limiting location, the cold leg and reactor coolant pump outlet nozzle junction, are given in Figure 5, which will be discussed further in the next section. For this location, the material of interest is the wrought seamless pipe material (SA 376 304N). The fracture properties of this material are equivalent to the data reported in Reference 1. Cast pipe (SA 351-CF8A) fittings, such as elbows, are subject to thermal aging. For this reason, an additional location with cast material properties was evaluated. This location is the junction between the cast elbow fitting and wrought pipe section at the inlet of the steam generator.

The fracture properties of CF8A cast stainless steel have been determined through fracture tests carried out at 600°F and reported in Reference 12. This reference shows that J_{IN} for the base metal ranges from [ ]^{a,c,e} for the multiple tests carried out.

Cast stainless steels are subject to thermal aging during service. This thermal aging causes an elevation in the yield strength of the material and a degradation of the fracture toughness, the degree of degradation being proportional to the level of ferrite in the material. To determine the effects of thermal aging on piping integrity a detailed study was carried out in Reference 13. In this report, fracture toughness results were presented for a material representative of [ ]^{a,c,e} Toughness results were provided for the material in the fully aged condition and these properties are also presented in Figure 4 of this report for information. The J_{IN} value for this material at operating temperature was approximately [ ]^{a,c,e} and the maximum value of J obtained in the tests was in excess of [ ]^{a,c,e} The tests of this material were conducted on small specimens and therefore rather short crack extensions, (maximum extension 4.3 mm) so it is expected that higher J values would be sustained for larger specimens. [

]^{a,c,e}

Therefore it may be concluded that the degree of thermal aging expected by end-of-life for these units is much less than that which was produced in [ ]^{a,c,e} of Reference 13, and therefore the J_{IN} values for the Byron/Braidwood plants 1 and 2 after end-of-life would be expected to be higher than those reported for [ ]^{a,c,e} in Figure 4 (Reference 14). In addition, the tearing modulus for the Byron/Braidwood Units 1 and 2 materials would be greater than [ ]^{a,c,e}

Available data on stainless steel welds indicate the J_{IN} values for the worst case welds are of the same order as the aged material, but the slope of the J-R curve is steeper, and higher J-values have been obtained from fracture tests (in excess of 3000 in-lb/in^2). The applied value of J integral for a flaw in the weld regions will be lower than that in the base metal because the yield stress for the weld materials is much higher at temperature. Therefore, weld regions are less limiting than the cast material.

4.4 Results of Crack Stability Evaluation

Figure 5 shows a plot of the [ ]^{a,c,e} as a function of through-wall circumferential flaw length in the [ ]^{a,c,e} of the main coolant piping. This [ ]^{a,c,e} was calculated for Byron/Braidwood data of a pressurized pipe at [ ]^{a,c,e} properties. The maximum applied bending moment of [ ]^{a,c,e} in-kips can be plotted on this figure, and used to determine the critical flaw length, which is shown to be [ ]^{a,c,e} inches. This is considerably larger than the [ ]^{a,c,e} inch reference flaw used in Reference 1.

[

]^{a,c,e} The maximum applied moment load for the present case is only 69 percent of the loads used in Reference 1. [

]^{a,c,e} Therefore, it can be concluded that a postulated [ ]^{a,c,e} inch through-wall flaw in the Byron/Braidwood plants loop piping will remain stable from both a local and global stability standpoint.

The J integral value was estimated for a [ ]^{a,c,e} long through-wall flaw. The estimation was based on extrapolation of the available finite element solution (Reference 1) for a [ ]^{a,c,e} long flaw. The amplification factor for estimating J corresponding to the larger crack was obtained by determining the J integrals using simplified handbook methods (Reference 19) for the two cracks when Reference 1 maximum loads were applied. This ampli-

fication factor was determined to be [ ].[a,c,e] Since the J value for a [ ][a,c,e] crack corresponding to the maximum Byron/Braidwood loads is [ ][a,c,e] the J_{app} for a 9 inch flaw is estimated to be about [ ].[a,c,e] This is within the range of the maximum J obtained in tests on wrought materials (Reference 1). The applied tearing modulus [ ][a,c,e] for a [ ][a,c,e] crack is significantly lower than the T_{mat} [ ][a,c,e] (Reference 1). Therefore, a postulated [ ][a,c,e] flaw will remain stable.

As an additional investigation to determine the sensitivity of J to flaw size, a [ ][a,c,e] through-wall flaw was analyzed. Here the maximum applied J was found to be less than [ ][a,c,e] in-lb/in^2.

At location 4 (see Figure 2), the maximum bending moment is [ ][a,c,e] and the axial force is [ ].[a,c,e] For this loading condition and the [ ][a,c,e] reference flaw size, a J value of less than [ ][a,c,e] would be expected. The applied tearing modulus $T_{applied}$ as taken from Reference 13 is [ ].[a,c,e] As stated in the previous section, the estimated tearing modulus for Byron and Braidwood (cast stainless steel elbows in the fully aged condition is at least [ ].[a,c,e] Therefore, a postulated [ ][a,c,e] flaw at location 4 will also remain stable.

At location 12 (see Figure 2), the thickness of the weld region is greater than the pipe thickness resulting in lower applied stress. Further, the yield stress for the weld material is much higher than the base metal (Reference 6). Therefore, the applied value of the J integral for a postulated flaw in the weld region will be significantly lower than [ ][a,c,e] in-lb/in^2 for the base metal.

5.0 LEAK RATE PREDICTIONS

Leak rate estimates were performed by applying the normal operating bending moment of [ ]^{a,c,e} in addition to the normal operating axial force of [ ]^{a,c,e} These loads were applied to the cold leg pipe containing a postulated [ ]^{a,c,e} through-wall flaw and the crack opening area was estimated using the method of Reference 15. The leak rate was calculated using the two-phase flow formulation described in Reference 1. The computed leak rate was [ ].^{a,c,e} In order to determine the sensitivity of leak rate to flaw size, a through-wall flaw [ ]^{a,c,e} in length was postulated. The calculated leak rate was [ ].^{a,c,e}

The Byron/Braidwood plants have an RCS pressure boundary leak detection system which is consistent with the guidelines of Regulatory Guide 1.45 of detecting leakage of 1 gpm in one hour. Thus, for the [ ]^{a,c,e} inch flaw, a factor of approximately [ ]^{a,c,e} exists between the calculated leak rate and the criteria of Regulatory Guide 1.45. Relative to the [ ]^{a,c,e}

6.0 FATIGUE CRACK GROWTH ANALYSIS

To determine the sensitivity of the primary coolant system to the presence of small cracks, a fatigue crack growth analysis was carried out for the [ ]^{a,c,e} region of a typical system. This region was selected because it is typically one of the highest stressed cross sections, and crack growth calculated here will be conservative for application to the entire primary coolant system.

A finite element stress analysis was carried out for the [ ]^{a,c,e} of a plant typical in geometry and operational characteristics to any Westinghouse PWR System. [

]^{a,c,e}

All normal, upset, and test conditions were considered and circumferentially oriented surface flaws were postulated in the region, assuming the flaw was located in three different locations, as shown in Figure 6. Specifically, these were:

[ ]^{a,c,e}

Fatigue crack growth rate laws were used [

]^{a,c,e} The law for stainless steel was derived from Reference 13, with a very conservative correction for R ratio, which is the ratio of minimum to maximum stress during a transient.

The law is:

$$\frac{da}{dn} = (5.4 \times 10^{-12})\ K_{eff}^{4.48} \text{ inches/cycle}$$

where $K_{eff} = K_{max}\ (1-R)^{0.5}$

$R = K_{min}/K_{max}$

[

]a,c,e

[ ] a,c,e

where:[ ] a,c,e

The calculated fatigue crack growth for semi-elliptic surface flaws of circumferential orientation and various depths is summarized in Table 2, and shows that the crack growth is very small, regardless [
]a,c,e

7.0 ASSESSMENT OF MARGINS

In Reference 1, the maximum design load was [ ]^{a,c,e} in-kips, whereas, the maximum load as noted in Section 3.0 of this report is significantly less, [ ]^{a,c,e} in-kips. For the current application, the maximum value of J [ ]^{a,c,e} in-lb/in^2 as determined by [ ]^{a,c,e} analyses compared with the value of [ ]^{a,c,e} in-lb/in^2 in Reference 1. Furthermore, Section 4.3 shows that the testing of fully aged material of chemistry worse than that existing in Byron/Braidwood plants cast piping extended to J values of [ ]^{a,c,e} in-lb/in^2; this is greater than the maximum value of applied J of [ ]^{a,c,e} in-lb/in^2 at cast stainless steel elbows. At maximum load the Byron/Braidwood plants Units 1 and 2 applied J-value is enveloped by the J_{max} of Reference 1. For cast elbows, the applied J-value is enveloped by the J_{max} value used in testing fully aged material.

In Section 4.4, it is seen that a [ ]^{a,c,e} flaw has a J value at maximum load of [ ] in-lb/in^2 which is also enveloped by the J_{max} value used for testing of wrought material. In Section 4.4, the "critical" flaw size using [ ]^{a,c,e} methods is calculated to be [ ]^{a,c,e} inches. Based on the above, the "critical" flaw size will, of course, exceed [ ]^{a,c,e}

Again, referring to Section 4.3, the estimated tearing modulus for Byron/Braidwood Units 1 and 2 cast SS piping in the fully aged condition is at least [ ].^{a,c,e} T_{app} as taken from Reference 13 is [ ].^{a,c,e} Consequently, a margin on local stability of at least [ ]^{a,c,e} exists relative to tearing. (The margin relative to tearing modulus in wrought material is considerably greater).

In Section 5.0, it is shown that a flaw of less than [ ]^{a,c,e} would yield a leak rate of [ ]^{a,c,e} Thus there is a factor of at least 3 between the minimum flaw size that gives a leak rate of [ ]^{a,c,e} and the "critical" flaw size of [ ].^{a,c,e}

In summary, relative to

1. Loads

   a. Byron/Braidwood Unit 1 and 2 are enveloped both by the maximum loads and J values in Reference 1 and the J values employed in testing of fully aged material and the forged material properties at the critical location.

   b. At the critical location, a margin of [ ]^{a,c,e} on faulted condition stresses and a margin of [ ]^{a,c,e} on thermal stresses exists relative to ASME code allowable values.

2. Flaw Size

   a. A margin of at least [ ]^{a,c,e} exists between the "critical" flaw and the flaw yielding a leak rate that meets the requirements of R.G. 1.45.

   b. A margin exists of at least [ ]^{a,c,e} relative to tearing.

   c. A margin exists of at least [ ]^{a,c,e} relative to global stability. If [ ]^{a,c,e} is used as the basis for "critical" flaw size, the margin for global stability would be at least [ ]^{a,c,e} with respect to a flaw size meeting the leak rate requirement of Regulatory Guide 1.45.

3. Leak Rate

   A margin of at least [ ]^{a,c,e} exists between calculated leak rates for the reference flaw and the criteria of Regulatory Guide 1.45.

8.0 CONCLUSIONS

This report has established the applicability of the generic Westinghouse evaluations which justify the elimination of RCS primary loop pipe breaks for the Byron/Braidwood plants as follows:

a. The loads, material properties, transients, and geometry relative to the Byron/Braidwood Units 1 and 2 RCS primary loop are enveloped by the parameters of WCAP-9558, Revision 2 (Reference 1) and WCAP-10456 (Reference 16).

b. Stress corrosion cracking is precluded by use of fracture resistant materials in the piping system and controls on reactor coolant chemistry, temperature, pressure, and flow during normal operation.

c. Water hammer should not occur in the RCS piping because of system design, testing, and operational considerations.

d. The effects of low and high cycle fatigue on the integrity of the primary piping are negligible.

e. Ample margin exists between the leak rate of the reference flaw and the criteria of Reg. Guide 1.45.

f. Ample margin exists between the reference flaw chosen for leak detectability and the "critical" flaw.

g. Ample margin exists in the material properties used to demonstrate end-of-life (relative to aging) stability of the reference flaw.

The reference flaw will be stable throughout reactor life because of the ample margins in e, f, and g, above, and will leak at a detectable rate which will assure a safe plant shutdown.

Based on the above, it is concluded that RCS primary loop pipe breaks should not be considered in the structural design basis of the Byron/Braidwood plants.

9.0 REFERENCES

1. WCAP-9558, Rev. 2, "Mechanistic Fracture Evaluation of Reactor Coolant Pipe Containing a Postulated Circumferential Through-Wall Crack," Westinghouse Proprietary Class 2, June 1981.

2. USNRC Generic letter 84-04, Subject: "Safety Evaluation of Westinghouse Topical Reports Dealing with Elimination of Postulated Pipe Breaks in PWR Primary Main Loops", February 1, 1984.

3. WCAP-8082 P-A, "Pipe Breaks for the LOCA Analysis of the Westinghouse Primary Coolant Loop," Class 2, January 1975.

4. Letter from Westinghouse (E. P. Rahe) to NRC (R. H. Vollmer), NS-EPR-2768, dated May 11, 1983.

5. WCAP-9283, "The Integrity of Primary Piping Systems of Westinghouse Nuclear Power Plants During Postulated Seismic Events," Westinghouse Proprietary Class 2, March, 1978.

6. WCAP-9787, "Tensile and Toughness Properties of Primary Piping Weld Metal for Use in Mechanistic Fracture Evaluation", Westinghouse Proprietary Class 2, May 1981.

7. Letter Report NS-EPR-2519, Westinghouse (E. P. Rahe) to NRC (D. G. Eisenhut), Westinghouse Proprietary Class 2, November 10, 1981.

8. Letter from Westinghouse (E. P. Rahe) to NRC (W. V. Johnson) dated April 25, 1983.

9. Letter from Westinghouse (E. P. Rahe) to NRC (W. V. Johnston) dated July 25, 1983.

10. NUREG-0691, "Investigation and Evaluation of Cracking Incidents in Piping in Pressurized Water Reactors", USNRC, September 1980.

11. Kanninen, M. F., et. al., "Mechanical Fracture Predictions for Sensitized Stainless Steel Piping with Circumferential Cracks", EPRI NP-192, September 1976.

12. Bush, A. J., Stoofer, R. B., "Fracture Toughness of Cast 316 SS Piping Material Heat No. 156576, at 600°F", W R D Memo No. 83-5P6EVMTL-M1, Westinghouse Proprietary Class 2, March 7, 1983.

13. WCAP-10456, "The Effects of Thermal Aging on the Structural Integrity of Cast Stainless Steel Piping For W NSSS," W Proprietary Class 2, November 1983.

14. Slama, G., Petrequin, P., Masson, S. H., and Mager, T. R., "Effect of Aging on Mechanical Properties of Austenitic Stainless Steel Casting and Welds", presented at SMiRT 7 Post Conference Semirar 6 - Assuring Structural Integrity of Steel Reactor Pressure Boundary Components, August 29/30, 1983, Monterey, CA.

15. NUREG/CR-3464, 1983, "The Application of Fracture Proof Design Methods using Tearing Instability Theory to Nuclear Piping Postulating Circumferential Through Wall Cracks"

16. Bamford, W. H., "Fatigue Crack Growth of Stainless Steel Piping in a Pressurized Water Reactor Environment", Trans. ASME Journal of Pressure Vessel Technology, Vol. 101, Feb. 1979.

17. [ ] a,c,e

18. [ ] a,c,e

19. Kumar, V., German, M. D., and Shih, C. F., "An Engineering Approach for Elastic-Plastic Fracture Analysis", EPRI, NP-1931.

TABLE 1

BYRON/BRAIDWOOD PLANTS PRIMARY LOOP DATA

[a,c,e

T-1

]

TABLE 2

FATIGUE CRACK GROWTH AT [ ]a,c,e (40 YEARS)

	FINAL FLAW (in)		
	[ ]a,c,e		
INITIAL FLAW (IN)	STEEL	[ ]a,c,e	[ ]a,c,e
0.292	0.31097	0.30107	0.30698
0.300	0.31949	0.30953	0.31626
0.375	0.39940	0.38948	0.40763
0.425	0.45271	0.4435	0.47421

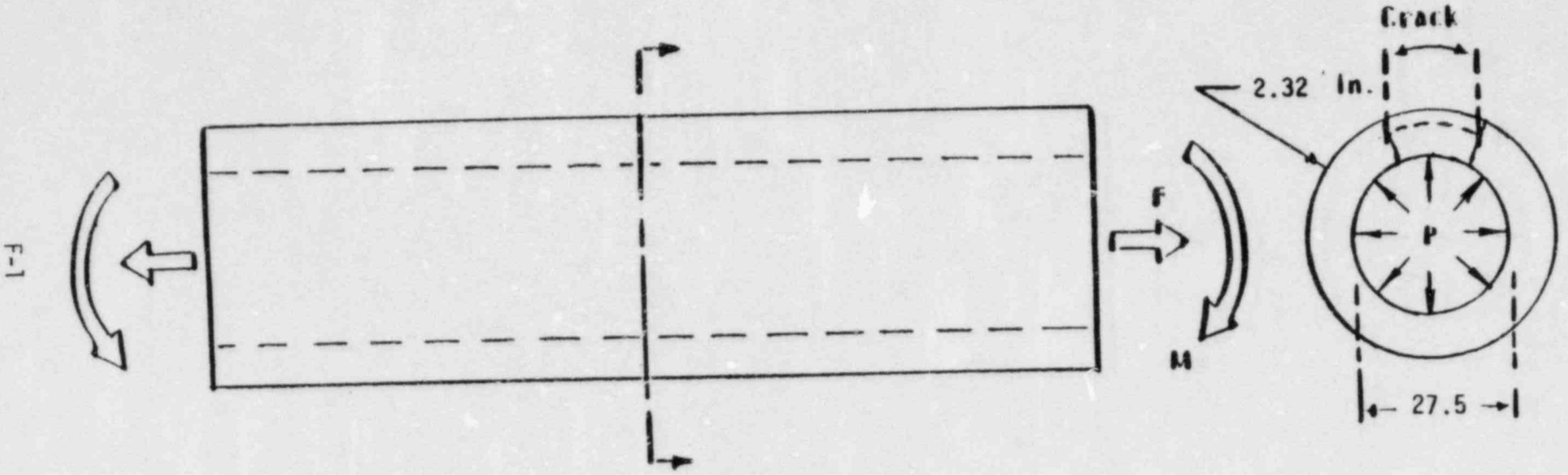

[ ] a,c,e

FIGURE 1 REACTOR COOLANT PIPE

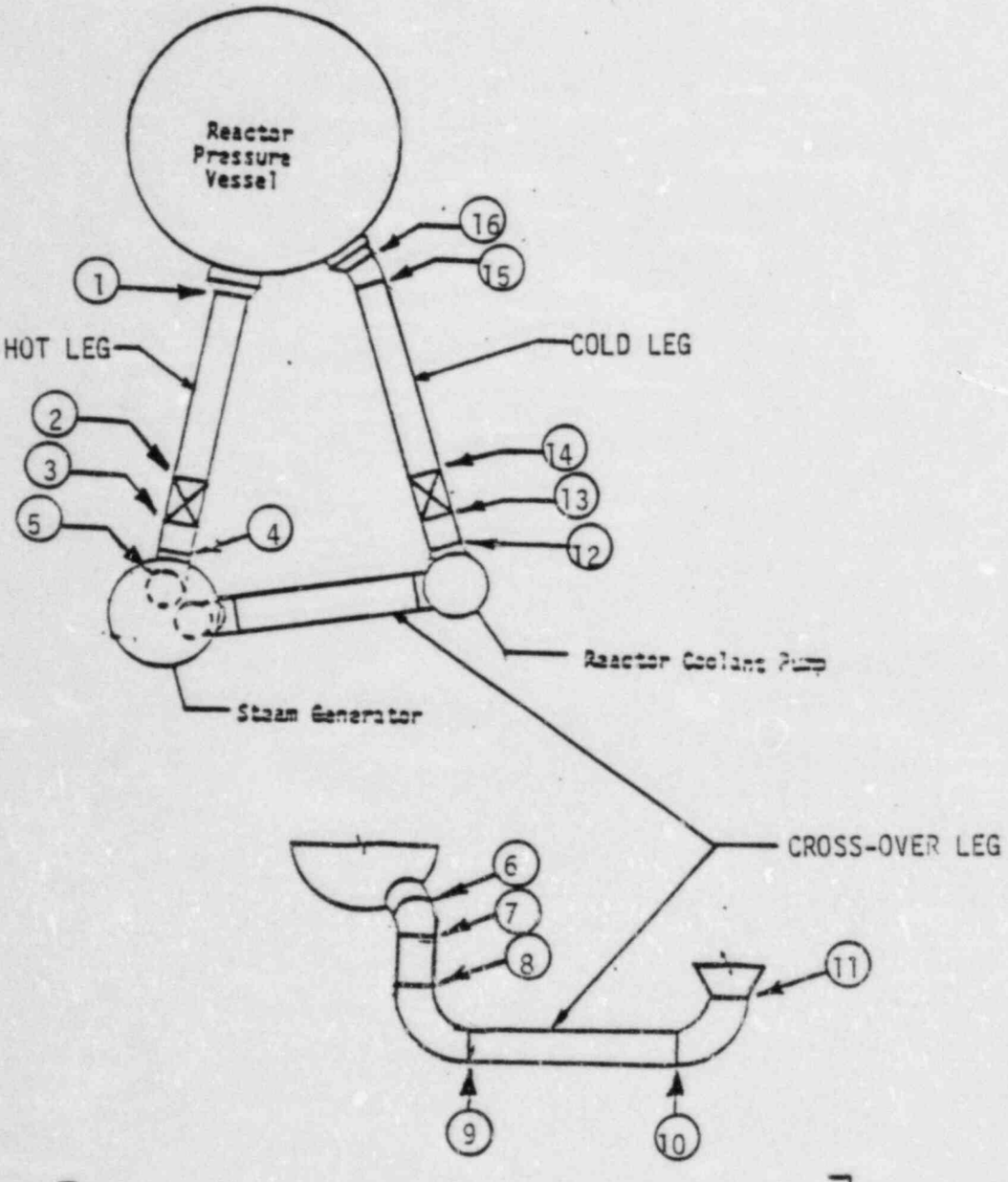

[ ] a,c,e

FIGURE 2 SCHEMATIC DIAGRAM OF PRIMARY LOOP SHOWING WELD LOCATIONS

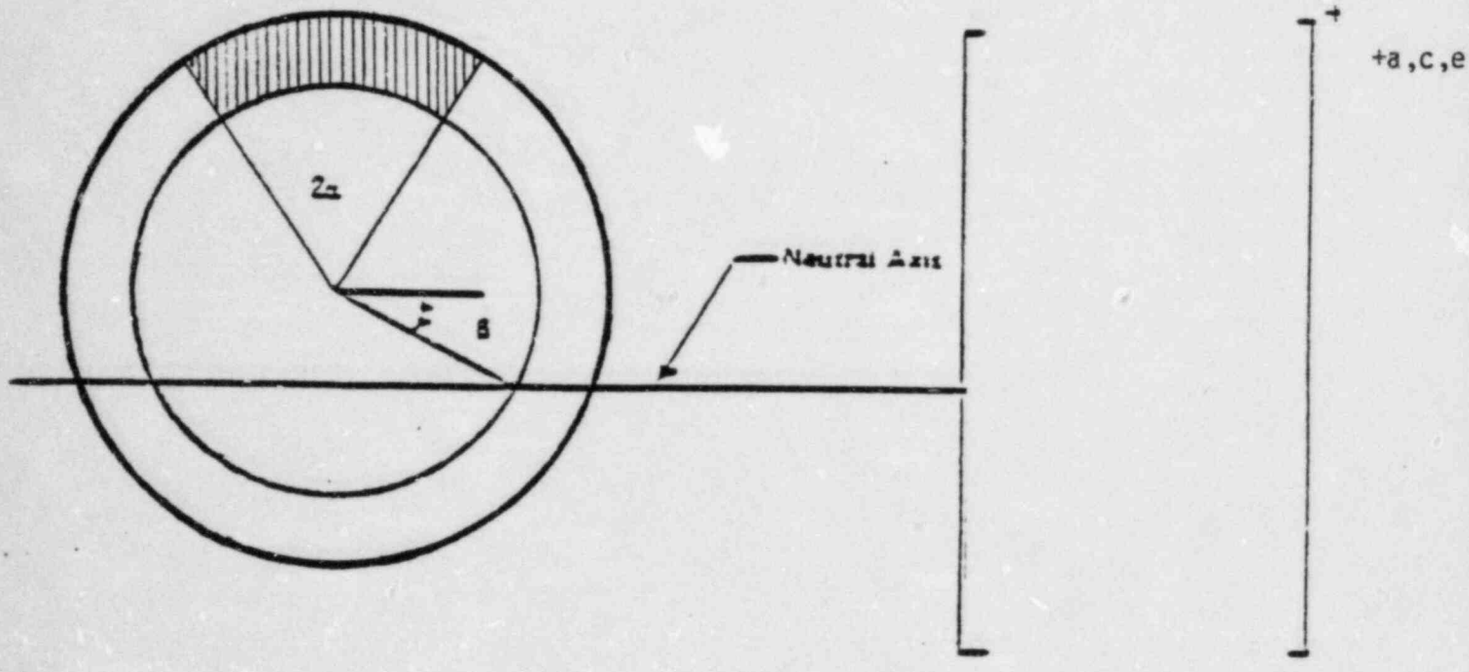

FIGURE 3 [ ] STRESS DISTRIBUTION ^{a,c,e}

FIGURE 4 J-Δa CURVES AT DIFFERENT TEMPERATURES. AGED MATERIAL [ ] a,c,e
(7500 HOURS AT 400°C)

Figure 5 Critical Flaw Size Prediction

FIGURE 6 TYPICAL CROSS SECTION OF [ ]+a,c,e

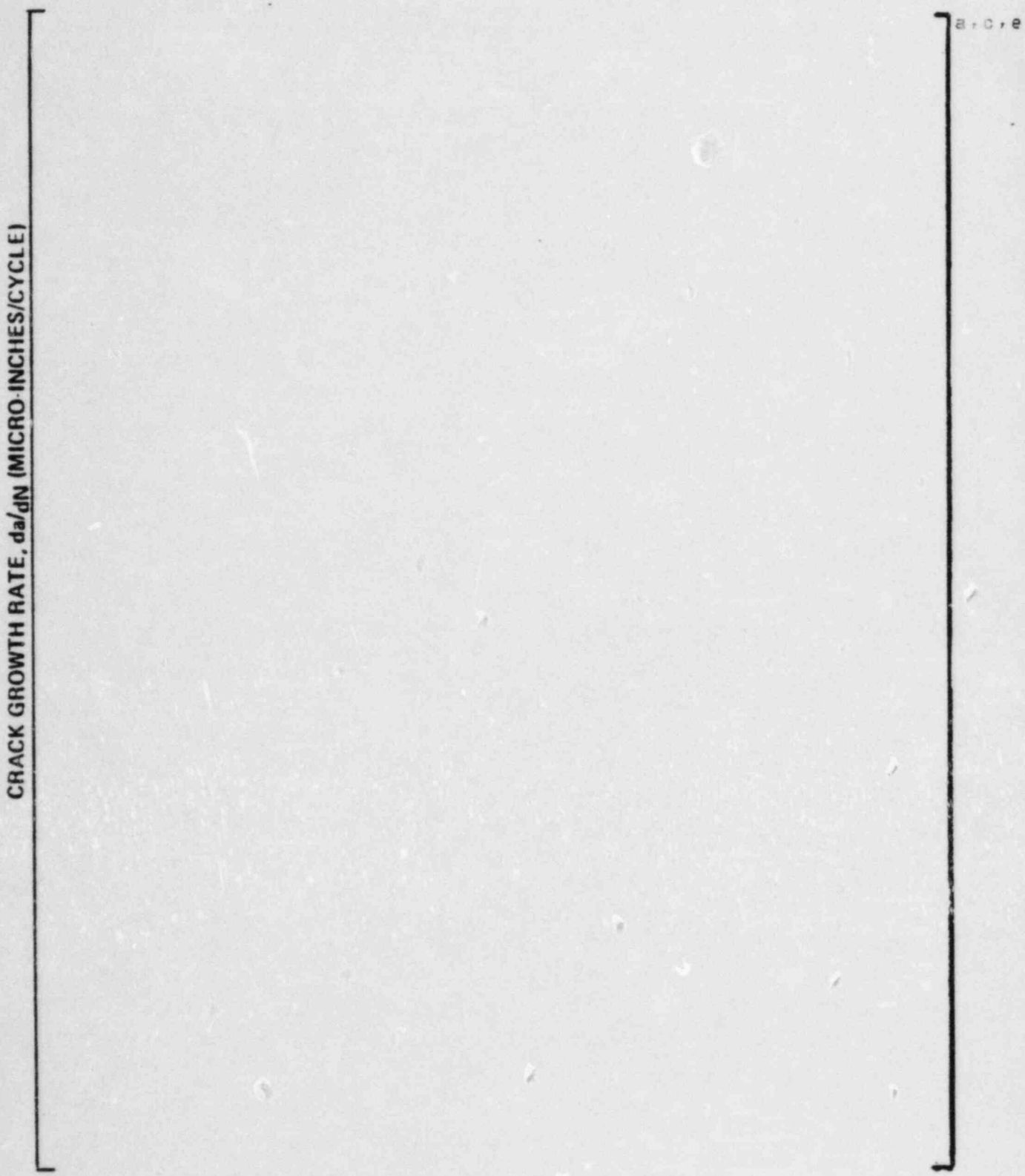

FIGURE 7. REFERENCE FATIGUE CRACK GROWTH CURVES FOR [ ] a,c,e

a,c,e

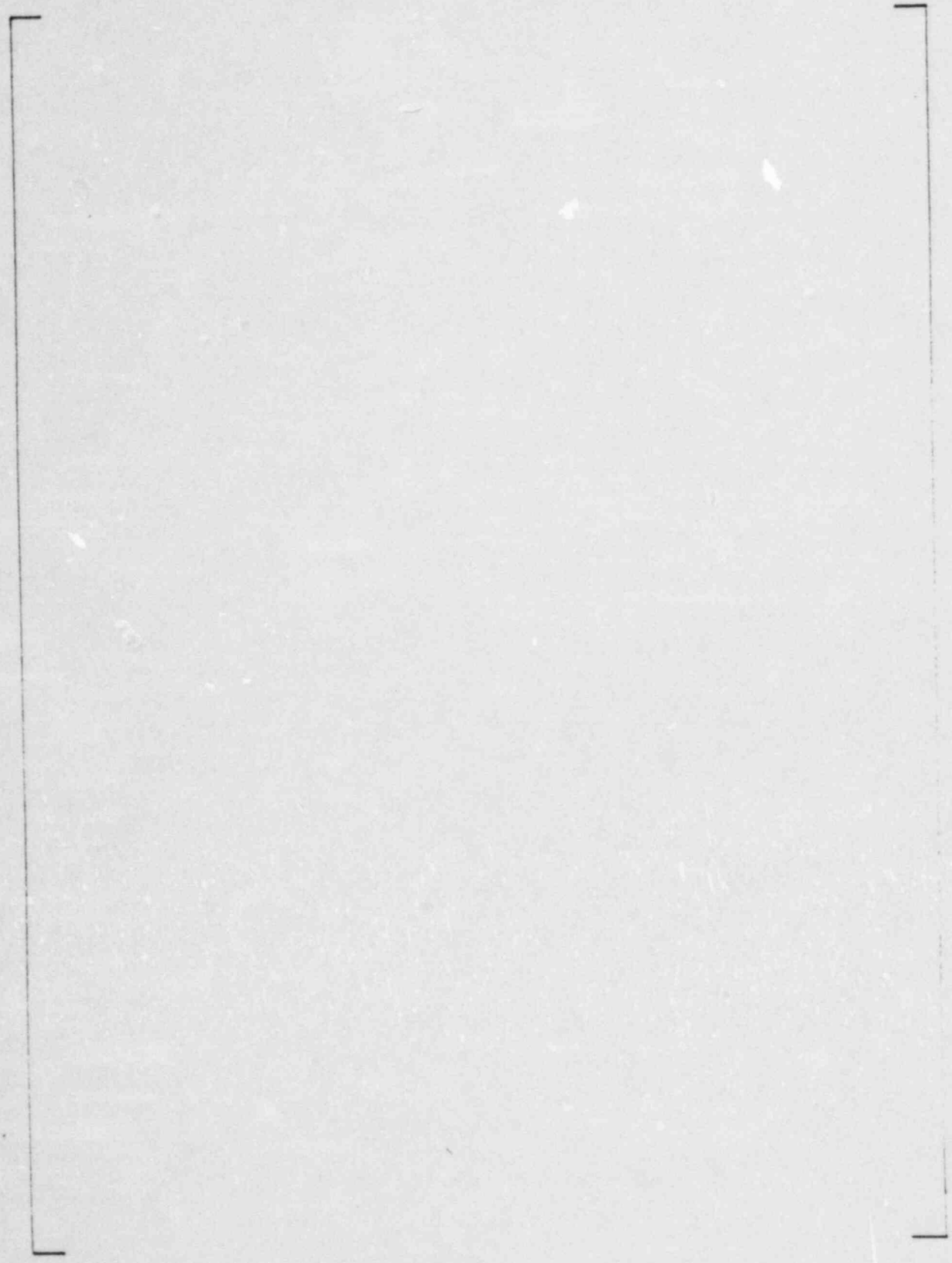

FIGURE 8 REFERENCE FATIGUE CRACK GROWTH LAW FOR [ ] a,c,e
IN A WATER ENVIRONMENT AT 600F

APPENDIX A

[a,c,e]

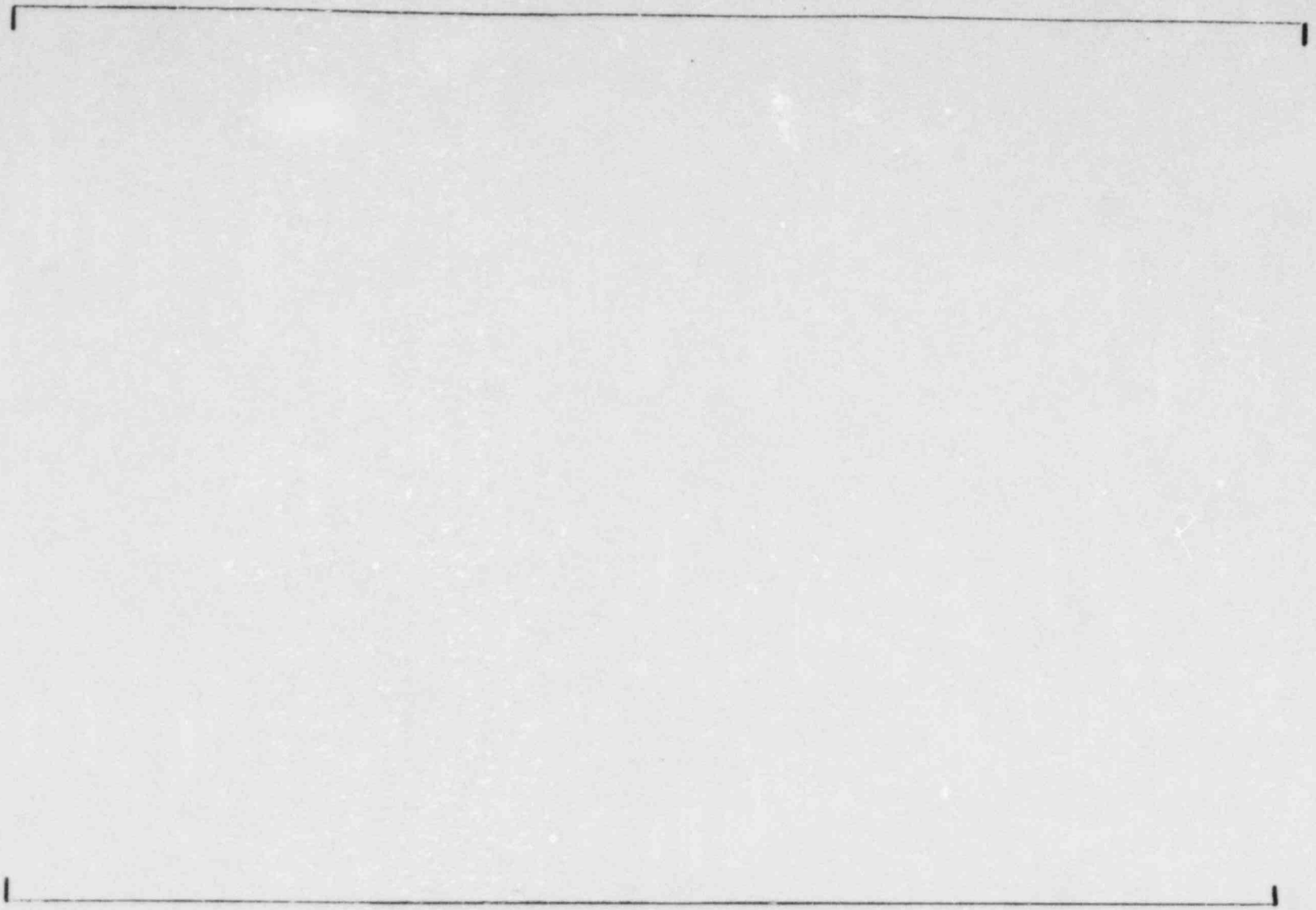

FIGURE A-1 PIPE WITH A THROUGH-WALL CRACK IN BENDING